JOURNAL OF CHEMICAL & ENGINEERING DATA

ARTICLE

pubs.acs.org/jced

Application of Aqai Stalks As Biosorbents for the Removal of the Dyes Reactive Black 5 and Reactive Orange 16 from Aqueous Solution

Natali F. Cardoso, Eder C. Lima,* Tatiana Calvete, Isis S. Pinto, Camila V. Amavisca, Thais H. M. Fernandes, Rodrigo B. Pinto, and Wagner S. Alencar

Institute of Chemistry, Federal University of Rio Grande do Sul, UFRGS, Av. Bento Gonçalves 9500, Postal Box 15003, 91501-970 Porto Alegre, RS, Brazil

Supporting Information

ABSTRACT: The aqai palm stalk (*Euterpe oleracea*) is a food residue used in its natural form (AS) and also protonated (AAS) as biosorbents for the removal of the textile dyes C.I. Reactive Black 5 and C.I. Reactive Orange 16 from aqueous solutions. This biosorbent was characterized by infrared spectroscopy, scanning electron microscopy, and nitrogen adsorption/desorption curves. The effects of pH, biosorbent dosage, and shaking time on the biosorption capacities were studied. In the acidic pH region (pH 2.0), the biosorption of the dyes was favorable. The contact time to obtain the equilibrium at 298 K was fixed at (10 and 4) h for the AS and AAS biosorbents, respectively, using both dyes. The Avrami fractionary-order kinetic model provided the best fit to the experimental data compared with the pseudofirst-order and pseudosecond-order kinetic adsorption models. The equilibrium data were fitted to the Langmuir, Freundlich, and Sips isotherm models. For both dyes the equilibrium data were best fitted to the Sips isotherm model.

INTRODUCTION

Dyes are one of the most hazardous chemical compound classes found in industrial effluents which need to be treated since their presence in water bodies reduces light penetration, precluding the photosynthesis of aqueous flora.[1,2] They are also aesthetically objectionable for drinking and other purposes.[3] Dyes can also cause allergy, dermatitis, and skin irritation[4] and also provoke cancer and cell mutations in humans.[5,6]

There are some methods that are used for treating waters containing dyes, such as, coagulation and flocculation,[7] degradation by visible light assisted by photocatalytic ozonation,[8] photocatalytic oxidation,[9] oxidative decomposition using the Fenton process,[10] catalytic wet air oxidation,[11] electrochemical degradation,[12] biological treatment with microorganisms.[13] However, all these processes lead to the formation of other byproducts that require continuous monitoring and identification, besides of most of them are expensive for treatment on a large scale.[14] One of the most employed methods for the removal of synthetic dyes from aqueous effluents is the adsorption procedure.[15,16] This process transfers the dyes from the water effluent to a solid phase, decreasing remarkably the dye bioavailability to live organisms. The decontaminated effluent could then be released to the environment or the water could be reutilized in the industrial process. Subsequently, the adsorbent can be regenerated or stored in a dry place without direct contact with the environment.[15,16]

Activated carbon is the most employed adsorbent for dye removal from aqueous solution because of its excellent adsorption properties.[17−19] However, the extensive use of activated carbon for dye removal from industrial effluents is expensive, limiting its large application for wastewater treatment.[20,21] Therefore, there is growing interest in finding alternative low cost adsorbents for dye removal from aqueous solution. These alternative adsorbents, include: helzenet shell,[21] saw dust wallnut,[21] saw dust cherry,[21] saw dust oak,[21] saw dust pitch pine,[21] saw dust pine,[21] cane pitch,[21] soy meal hull,[21] banana pitch,[21] sugar cane bagasse,[20] cotton waste,[20] chitin and chitosan,[20] peat,[20] microorganisms such as fungus and yeasts,[20] maize cob,[20,21] and Brazilian pine-fruit shell.[15,22,23]

Aqai palm (*Euterpe oleracea*) is native to the Brazilian Amazon; however, it has already been cultivated in the United States.[24] The palms of *E. oleracea* are multistemmed, monoecious, and may reach heights of > 25 m. The fruit, a small, round, black-purple drupe about 25 mm in circumference, is produced in branched panicles of (500 to 900) fruits.[25,26] Aqai pulp is utilized in the manufacture of a variety of foods and beverages.[25,26] The Brazilian annual production of aqai is about 160 000 tons.[27] About 20% of the weight of the aqai is the stalk (AS) that held its fruits, which is a waste material that presents no aggregate economic value.[27]

The disposal of large amounts of AS directly in the soil and/or in natural waters may contaminate the environment in an uncontrolled way because the decomposition of this waste material leads to the generation of various chemical compounds and microorganisms. In this context, combining the need to reduce costs with commercial adsorbents and by using AS as a biosorbent for the removal of dyes from industrial effluents, is a good economical and environmental advantage to developing countries such as Brazil.

The present work aimed to use aqai stalk in natural (AS) and protonated (AAS) forms as biosorbents for the successful removal

Received: August 21, 2010
Accepted: February 25, 2011
Published: March 14, 2011

ACS Publications © 2011 American Chemical Society

of the dyes C.I. Reactive Black 5 (RB-5) and C.I. Reactive Orange 16 (RO-16) from aqueous solutions. These dyes are largely used for textile dying in the Brazilian cloth industries.

MATERIALS AND METHODS

Solutions and Reagents. Deionized water was used throughout the experiments for solution preparations.

The textile dyes, C.I. Reactive Black 5 (C.I. 20505; CAS 12225-25-1; $C_{26}H_{21}N_5O_{19}S_6Na_4$, 991.82 g·mol^{-1}, λ_{max} = 590 nm, see Supporting Information, Figure 1) at 55% purity and C.I. Reactive Orange 16 (C.I. 17757; CAS 20262-58-2; $C_{20}H_{17}N_3O_{11}S_3Na_2$, 617.54 g·mol^{-1}, λ_{max} = 493 nm, see Supporting Information, Figure 1) at 50 % purity, both were furnished by Sigma-Aldrich (St. Louis, MO). The dyes were used without further purification. The RB-5 dye has two sulfonate groups and two sulfato-ethyl-sulfone groups, and the RO-16 has one sulfato-ethyl-sulfone group and one sulfonate group. These groups present negative charges even in highly acidic solutions due to their pK_a values that are lower than zero.[18,22] A stock solution was prepared by dissolving the dyes in distilled water to the concentration of 5.00 g·L^{-1}. Working solutions were obtained by diluting the dye stock solutions to the required concentrations. To adjust the pH solutions, 0.10 mol·L^{-1} sodium hydroxide or hydrochloric acid solutions were used. The pH of the solutions was measured using a Schott Lab 850 set pH meter.

Adsorbent Preparation and Characterization. AS was furnished by the ice cream industry in Belém-PA, Brazil, as a residual material. AS was washed with tap water to remove dust and with deionized water. Then, it was dried at 70 °C in an air-supplied oven for 8 h. After that, AS was grounded in a disk-mill and subsequently sieved. The part of the biosorbent which presented a diameter of particles ≤ 250 μm was used. This unmodified aqai stalk was assigned as AS.

In order to increase the amount adsorbed of RB-5 and RO-16 dyes by the AS biosorbent the biomaterial was protonated as described below.[22] An amount of 5.0 g of AS was added to 200.0 mL of 3 mol·L^{-1} of HCl, and the slurry was magnetically stirred for 24 h at 70 °C. Subsequently, the slurry was filtered in a sintered glass funnel, and the solid phase was thoroughly washed with water, until the filtrate reached the pH of distilled water. Subsequently, the material was dried at 70 °C in an air supplied oven for 8 h, yielding the acidified aqai stalk (AAS).

The AS and AAS biosorbents were characterized by FTIR using a Shimadzu FTIR, model 8300 (Kyoto, Japan). The spectra were obtained with a resolution of 4 cm^{-1}, with 100 cumulative scans.[28]

The surface analyses and porosity were carried out with a volumetric adsorption analyzer, ASAP 2020, from Micrometrics, at 77 K (boiling point of nitrogen). The samples were pretreated at 373 K for 24 h under a nitrogen atmosphere in order to eliminate the moisture adsorbed on the solid sample surface. After, the samples were submitted to 298 K in a vacuum, reaching the residual pressure of 10^{-4} Pa. For area and pore size distribution calculations, the BET and BJH methods were used.[29,30]

The AS and AAS biosorbent samples were also analyzed by scanning electron microscopy (SEM) in a Jeol microscope, model JSM 6060, using an acceleration voltage of 20 kV and magnification ranging from 100 to 5000 fold.[31]

Biosorption Studies. The biosorption studies for evaluation of the AS and AAS biosorbents for the removal of the RB-5 and RO-16 dyes from aqueous solutions were carried out in triplicate using the batch contact biosorption method. For these experiments, fixed amounts of biosorbent [(20.0 to 200.0) mg] were placed in 50 mL cylindrical high-density polystyrene flasks (117 mm height and 30 mm diameter) containing 20.0 mL of dye solutions [(10.00 to 300.0) mg·L^{-1}], which were agitated for a suitable time [(0.5 to 48) h] at 298 K. The pH of the dye solutions ranged from 2.0 to 10.0. Subsequently, in order to separate the biosorbents from the aqueous solutions, the flasks were centrifuged at 3600 rpm for 10 min, and aliquots of (1 to 10) mL of supernatant were properly diluted with water.

Table 1. Kinetic Adsorption Models

kinetic model	equation
fractionary-order	$q_t = q_e\{1 - \exp[-(k_{AV}t)]^{nAV}\}$
	$h_o = k_s q_e$
	initial sorption rate
pseudofirst order	$q_t = q_e[1 - \exp(-k_f t)]$
	$h_o = k_s q_e$
	initial sorption rate
pseudosecond order	$q_t = (k_s q_e^2 t)/(1 + q_e k_s t)$
	$h_o = k_s q_e^2$
	initial sorption rate
intraparticle diffusion	$q_t = k_{id}(t)^{1/2} + C$

Table 2. Equilibrium Models

isotherm model	equation
Langmuir	$q_e = (Q_{max}K_L C_e)/(1 + K_L C_e)$
Freundlich	$q_e = K_F C_e^{1/nF}$
Sips	$q_e = (Q_{max}(K_S C_e)^{1/ns})/(1 + (K_S C_e)^{1/ns})$

The final concentrations of the dyes remaining in the solution were determined by visible spectrophotometry using a T90+ UV−vis spectrophotometer furnished by PG Instruments (London-England) provided with quartz optical cells. Absorbance measurements were made at the maximum wavelength of RB-5 and RO-16 which were (590 and 493) nm, respectively.

The amount of dyes adsorbed and the percentage of removal of the dyes by the biosorbent were calculated by applying the eqs 1 and 2, respectively:

$$q = \frac{(C_o - C_f)}{X} \quad (1)$$

$$\% \text{ removal} = 100 \cdot \frac{(C_o - C_f)}{C_o} \quad (2)$$

where q is the amount of dyes adsorbed by the biosorbent (mg·g^{-1}), C_o is the initial dye concentration put in contact with the adsorbent (mg·L^{-1}), C_f is the dye concentration (mg·L^{-1}) after the batch adsorption procedure, and X is biosorbent dosage (g·L^{-1}).

Kinetic and Equilibrium Models. The Avrami fractionary-order,[32] pseudofirst-order,[33] pseudosecond-order,[34] and intraparticle diffusion model[35] kinetic equations are given in Table 1.

The Langmuir,[36] Freundlich,[37] and Sips[38] isotherm equations are given in Table 2.

Quality Assurance and Statistical Evaluation of the Kinetic and Isotherm Parameters. To establish the accuracy, reliability,

Table 3. FTIR Bands (cm^{-1}) of the Adsorbents AS and AAS before and after the Adsorption of RB-5 and RO-16 Dyes

wavenumber (cm^{-1})						
AS	AS+RB-5	AS+RO-16	AAS	AAS+RB-5	AAS+RO-16	assignments
3433	3427	3426	3431	3425	3419	O−H bond stretching[44,45]
1735	1730	1730	1734	1730	1730	stretching of carbonyl groups of carboxylic acid[45]
1252	1245	1246	1252	1241	1241	C−O stretch of phenolic compounds found in lignin[44,45]
1045	1033	1030	1057	1044	1046	C−O stretch of phenolic compounds found in lignin[44,45]

and reproducibility of the collected data, all of the batch adsorption measurements were performed in triplicate. Blanks were run in parallel and they were corrected when necessary.[39]

All dye solutions were stored in glass flasks, which were cleaned by soaking in 1.4 $mol \cdot L^{-1}$ HNO_3 for 24 h,[40] rinsing five times with deionized water, dried, and stored in a flow hood.

For analytical calibration, standard solutions with concentrations ranging from (5.00 to 50.0) $mg \cdot L^{-1}$ of the dyes were employed, running against a blank solution of water adjusted to pH 2.0. The linear analytical calibration of the curve was furnished by the UVWin software of the T90+ PG Instruments spectrophotometer. The detection limits of the method, obtained with a signal/noise ratio of 3,[41] were (0.18 and 0.11) $mg \cdot L^{-1}$, for RB-5 and RO-16, respectively. All of the analytical measurements were performed in triplicate, and the precision of the standards was better than 3 % ($n = 3$). For checking the accuracy of the RB-5 and RO-16 dye sample solutions during the spectrophotometric measurements, standards containing dyes at 5.00 $mg \cdot L^{-1}$ were employed as a quality control every five determinations.[42]

The kinetic and equilibrium models were fitted by employing a nonlinear method, with successive interactions calculated by the method of Levenberg−Marquardt and also interactions calculated by the Simplex method, using the nonlinear fitting facilities of the software Microcal Origin 7.0. In addition, the models were also evaluated by adjusted determination factor (R_{adj}^2), as well as by an error function (F_{error}),[43] which measures the differences in the amount of dye taken up by the adsorbent predicted by the models and the actual q measured experimentally. R_{adj}^2 and F_{error} are given below, in eqs 3 and 4, respectively

$$R_{adj}^2 = 1 - \left(\frac{\sum_i^n (q_{i,exp} - q_{i,model})^2}{\sum_i^n (q_{i,exp} - \overline{q}_{i,exp})^2} \right) \left(\frac{n-1}{n-p} \right) \quad (3)$$

$$F_{error} = \sqrt{\left(\frac{1}{n-p} \right) \sum_i^n (q_{i,exp} - q_{i,model})^2} \quad (4)$$

where $q_{i,model}$ is each value of q predicted by the fitted model, $q_{i,exp}$ is each value of q measured experimentally, $\overline{q}_{exp}$ is the average of q experimentally measured, n is the number of experiments performed, and p is the number of parameters of the fitted model.[43]

RESULTS AND DISCUSSION

Characterization of Biosorbents. The FTIR technique was used to examine the surface groups of the AS and AAS biosorbents and to identify the groups responsible for the dyes adsorption. Infrared spectra of the adsorbents and dye-loaded adsorbent samples, before and after the adsorption process, were recorded in the range (4000 to 400) cm^{-1} (see the Supporting Information, Figure 2A-F). Table 3 presents the significant changes of FTIR vibrational spectra of AS and AAS adsorbents before the adsorption and loaded with the RB-5 and RO-16 dyes after the adsorption. The FTIR band assignments are based on the literature.[44,45] As previously observed for an activated carbon[18,19] and a fly ash adsorbent[46] after the adsorption procedure, the functional groups that interact with the dye suffered a shift to lower wavenumbers when the adsorbate withdrew electrons of the adsorbent group. These FTIR results indicate that the interaction of RB-5 and RO-16 dyes with the AS and AAS biosorbents should occur with the O−H bonds of phenols and alcohols present in the lignin structure as well as interactions with the carboxylate group because these groups suffered a shift to lower wavenumbers after the biosorption procedure.

The textural properties of AS and AAS obtained by nitrogen adsorption/desorption curves were: superficial area (S_{BET}) (1.6 and 2.0) $m^2 \cdot g^{-1}$; average pore diameter (BJH) (10.77 and 11.80) nm; and total pore volume (0.0050 and 0.0077) $cm^3 \cdot g^{-1}$ for AS and AAS, respectively. The superficial area of agricultural residues is usually a low value.[47,48] On the other hand, the average pore diameter of AS and AAS biomaterials are relatively large, even when compared with activated carbons[17,18] or silicates.[2,3,16] The maximum diagonal lengths of the RB-5 and RO-16 (see the Supporting Information, Figure 1) are (2.55 and 1.68) nm, respectively. The ratios of average pore diameter of the biosorbents to the maximum diagonal length of each dye are 4.22 (ØAS/ØRB-5); 4.63 (ØAAS/ØRB-5); 6.41 (ØAS/ØRO-16); and 7.02 (ØAAS/ØRO-16). Therefore, the mesopores of the biosorbents could accommodate up to 4 molecules of RB-5 for AS and AAS and up to 6 molecules of RO-16 for AS and up to 7 molecules of RO-16 for AAS. This number of molecules, which could be accommodated in each pore of the biosorbent, is considered large when compared with other adsorbents reported in the literature.[17,18]

Scanning electron microscope (SEM) analysis results of the AS and AAS biosorbents without contact with the dye solution (Figure 1A,C for AS and AAS, respectively) and after contact with the RO-16 dye solution at pH 2.0 (Figure 1B,D for AS and AAS, respectively) are shown in Figure 1. As can be seen, for the AS biosorbent without contact with the dye solution is a more compact fibrous material (see Figure 1A). On the other hand, after the AS biosorbent has been in contact with an RO-16 dye solution at pH 2.0 for 4 h, some cavities of the fibrous materials appeared, which should allow the diffusion of dye molecules through the macropore (pore with Ø > 50 nm)[29,30] of the AS biosorbent. For the AAS biosorbent, the material already presents several macropore structures (see Figure 1C) and after the contact with RO-16 dye solution at pH 2.0 for 8 h, no significant differences were observed. Therefore, the acid

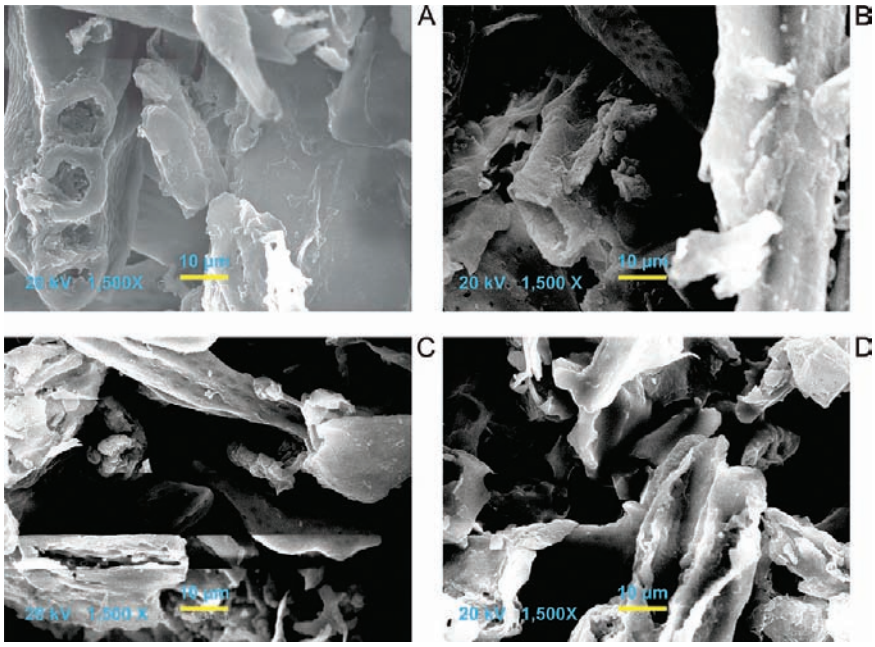

Figure 1. SEM of (A) AS without contact with dye solution, (B) AS after contact with RO-16 dye solution, (C) AAS without contact with dye solution, and (D) AAS after contact with RO-16 dye solution. Magnification 1500×; accelerating voltage 20 kV.

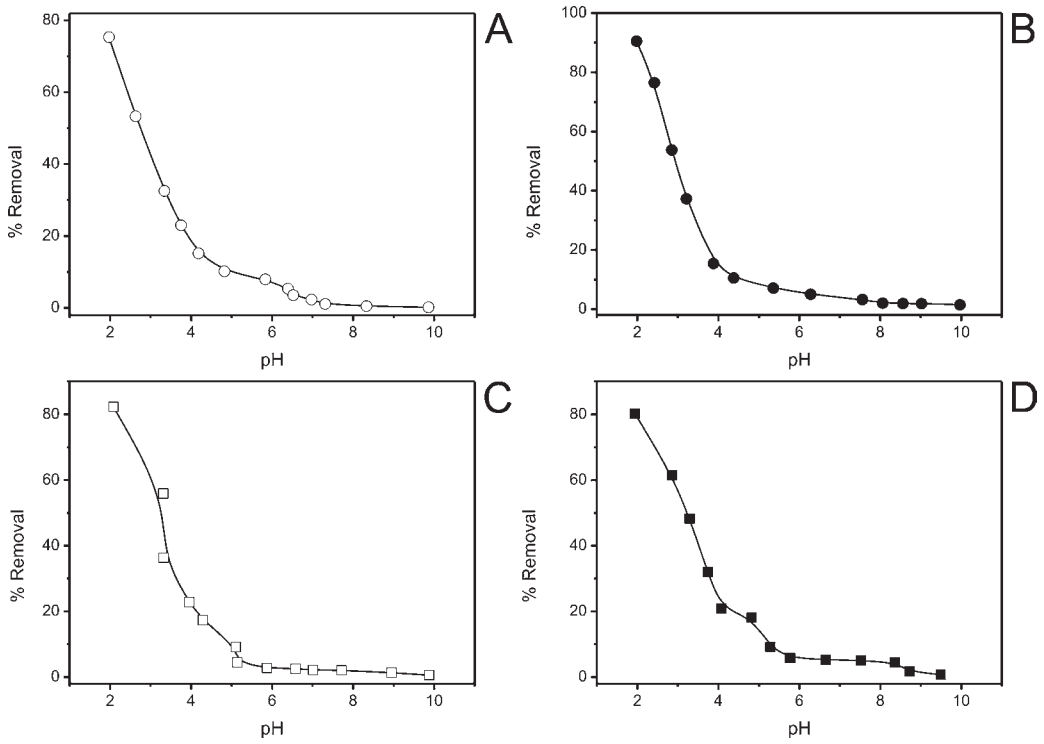

Figure 2. Effect of pH on the biosorption of (A) RB-5 on AS biosorbent, (B) RB-5 on AAS biosorbent, (C) RO-16 on AS biosorbent, and (D) RO-16 on AAS biosorbent. Conditions: C_o= 40.0 mg·L^{-1} of dye solution and mass of biosorbent of 30.0 mg for both dyes. The temperature was fixed at 298 K.

treatment of aqai fiber with 3.0 mol·L^{-1} HCl generated several macropores on the biomaterial fiber, which allowed the diffusion of the dyes by the pore of the biosorbent. By these results it is expected that the AAS biosorbent should present higher sorption capacity than the AS biosorbent, as already reported in the literature.[30] The macropores facilitate the diffusion of the dye molecules inside the fiber pores of the biosorbents (increasing the intraparticle diffusion). As the adsorbate diffuses through the pores of the biosorbent, the dye could be adsorbed at the internal sites of the biomaterial. On the other

dx.doi.org/10.1021/je100866c |*J. Chem. Eng. Data* 2011, 56, 1857–1868

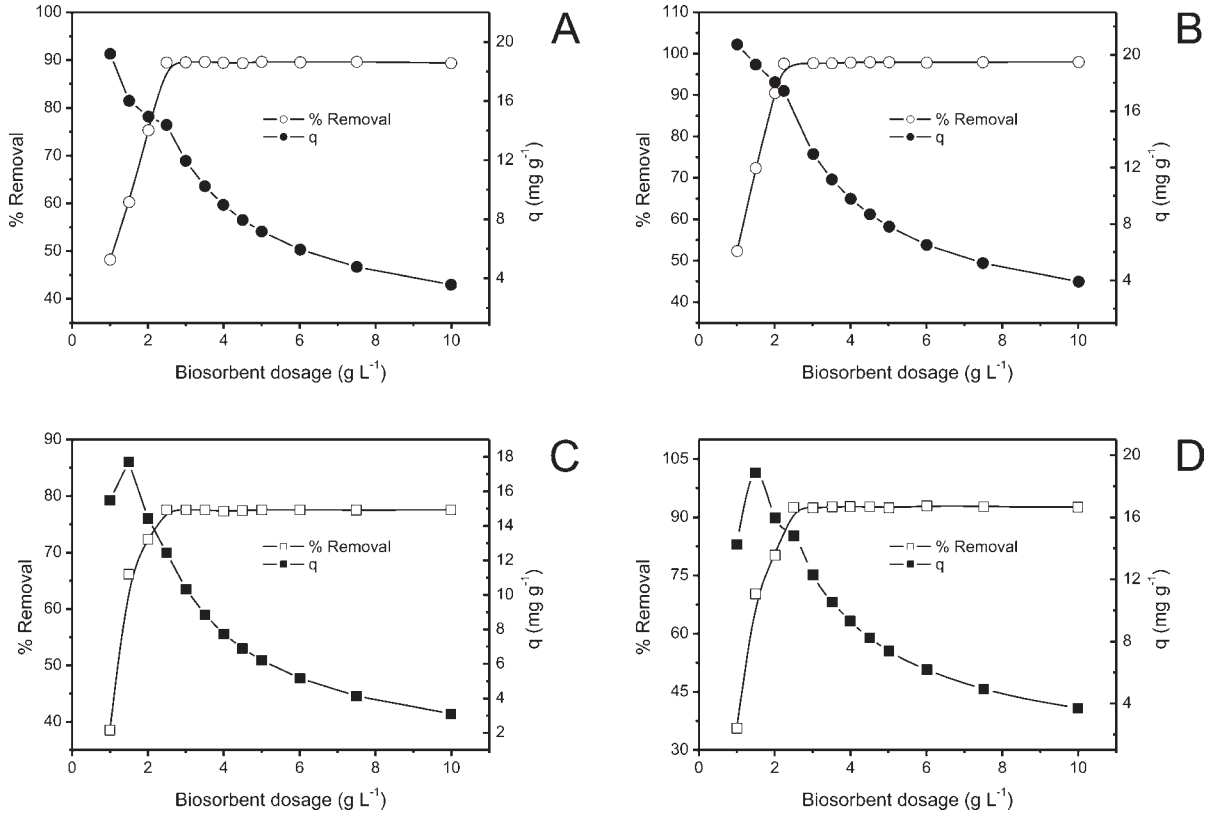

Figure 3. Effect of biosorbent dosage on the percentage of dye removal and amount of dye adsorbed. (A) RB-5 adsorbed on AS, (B) RB-5 adsorbed on AAS, (C) RO-16 adsorbed on AS, and (D) RO-16 adsorbed on AAS. Conditions: initial pH 2.0; C_o= 40.0 mg·L^{-1}; T = 298 K, time of contact 12 h.

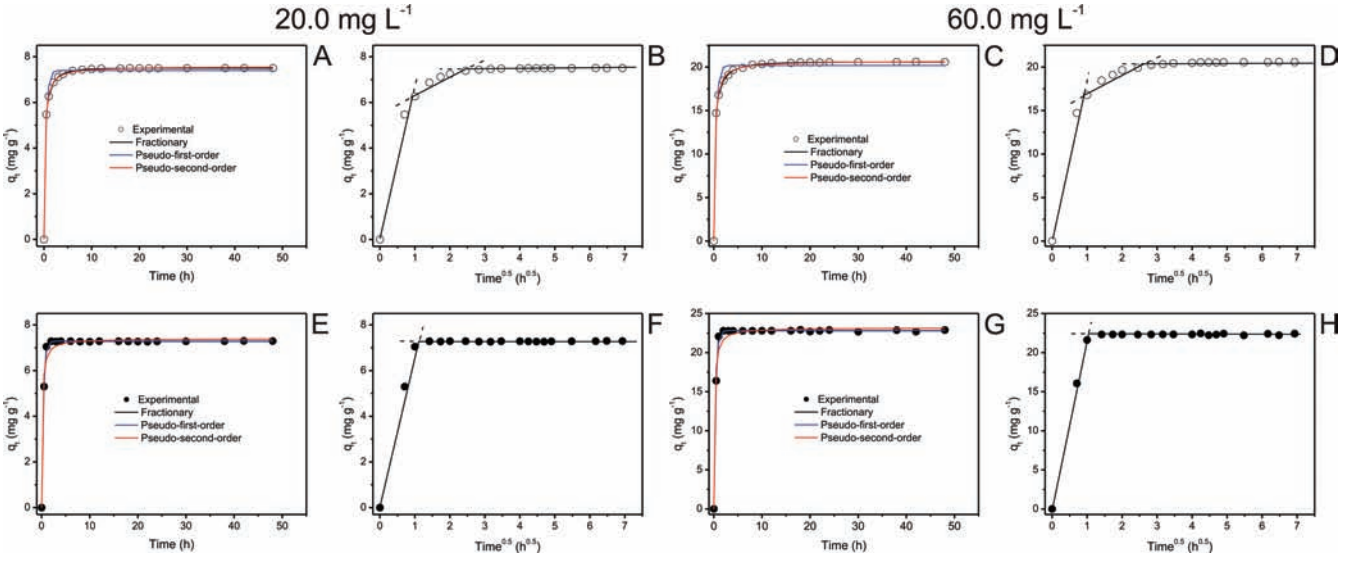

Figure 4. Kinetic biosorption curves of RB-5 dye. (A) Biosorbent AS; C_o 20.0 mg·L^{-1}; (B) intraparticle diffusion; biosorbent AS; C_o 20.0 mg·L^{-1}; (C) biosorbent AS; C_o 60.0 mg·L^{-1}; (D) intraparticle diffusion; biosorbent AS; C_o 60.0 mg·L^{-1}; (E) biosorbent AAS; C_o 20.0 mg·L^{-1}; (F) intraparticle diffusion; biosorbent AAS; C_o 20.0 mg·L^{-1}; (G) biosorbent AAS; C_o 60.0 mg·L^{-1}; (H) intraparticle diffusion; biosorbent AAS; C_o 60.0 mg·L^{-1}. Conditions: pH was fixed at 2.0; the biosorbent dosage was fixed at 2.5 g·L^{-1}; and the temperature was fixed at 298 K.

hand, the biosorbent with a lower number of macropore structures, the adsorption is limited to the external surface of the biosorbent, decreasing the total amount adsorbed.[30] Similar results were also obtained with RB-5 after the contact with AS and AAS biosorbents (data not shown).

Taking into account that AS and AAS biosorbents present low superficial areas (S_{BET}) and some macropores (see Figure 1), it could be inferred that AS and AAS predominate a mixture of mesopores (pores with diameters ranging from (2 to 50) nm, see textural results described above) and

dx.doi.org/10.1021/je100866c |J. Chem. Eng. Data 2011, 56, 1857–1868

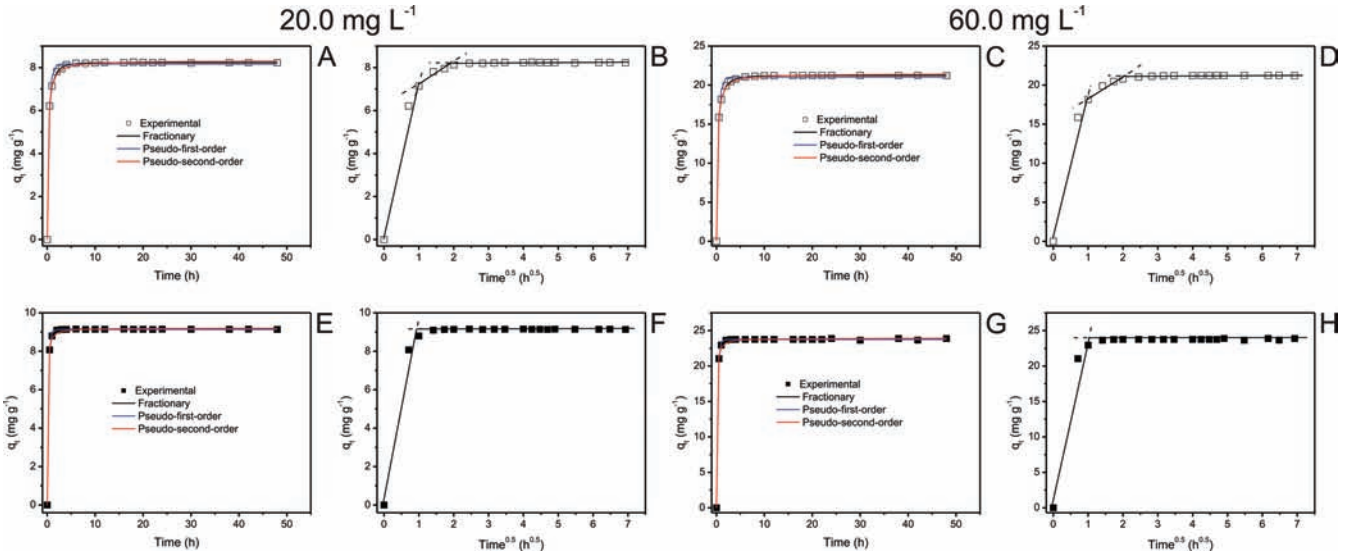

Figure 5. Kinetic biosorption curves of RO-16 dye. (A) Biosorbent AS; C_o 20.0 mg·L^{-1}; (B) intraparticle diffusion; biosorbent AS; C_o 20.0 mg·L^{-1}; (C) biosorbent AS; C_o 60.0 mg·L^{-1}; (D) intraparticle diffusion; biosorbent AS; C_o 60.0 mg·L^{-1}; (E) biosorbent AAS; C_o 20.0 mg·L^{-1}; (F) intraparticle diffusion; biosorbent AAS; C_o 20.0 mg·L^{-1}; (G) biosorbent AAS; C_o 60.0 mg·L^{-1}; (H) intraparticle diffusion; biosorbent AAS; C_o 60.0 mg·L^{-1}. Conditions: pH was fixed at 2.0; the biosorbent dosage was fixed at 2.5 g·L^{-1}; and the temperature was fixed at 298 K.

Table 4. Kinetic Parameters for RB-5 and RO-16 Removal Using AS and AAS as Biosorbents[a]

	AS				AAS			
	RB-5		RO-16		RB-5		RO-16	
	20 mg·L^{-1}	60 mg·L^{-1}	20 mg·L^{-1}	60 mg·L^{-1}	20 mg·L^{-1}	60 mg·L^{-1}	20 mg L^{-1}	60 mg L^{-1}
				Fractionary-Order				
k_{AV} (h^{-1})	3.57	3.44	3.84	3.79	2.41	2.36	6.84	6.72
q_e (mg·g^{-1})	7.50	20.6	8.23	21.2	7.28	22.3	9.15	23.8
n_{AV}	0.461	0.422	0.523	0.498	1.40	1.44	0.618	0.637
h_o (mg·g^{-1}·h^{-1})	26.8	70.9	31.6	80.5	17.6	52.8	62.5	159.8
R_{adj}^2	1.000	0.9999	0.9999	1.000	1.000	0.9998	1.000	0.9999
F_{error}	0.00459	0.0414	0.0188	0.0132	0.00972	0.0686	0.00786	0.0649
				Pseudofirst-Order				
k_f (h^{-1})	2.37	2.26	2.61	2.53	2.72	2.67	4.21	4.27
q_e (mg·g^{-1})	7.40	20.2	8.17	21.0	7.29	22.4	9.13	23.7
h_o (mg·g^{-1}·h^{-1})	17.6	45.6	21.3	53.3	19.9	59.8	38.5	101
R_{adj}^2	0.9861	0.9799	0.9928	0.9908	0.9985	0.9981	0.9994	0.9994
F_{error}	0.205	0.677	0.1615	0.4715	0.0663	0.231	0.0524	0.135
				Pseudosecond-Order				
k_s (g·mg^{-1}·h^{-1})	0.674	0.222	0.741	0.270	0.992	0.313	1.79	0.715
q_e (mg·g^{-1})	7.57	20.7	8.33	21.5	7.40	22.7	9.21	23.9
h_o (mg·g^{-1}·h^{-1})	38.6	95.3	51.4	124	54.3	161	152	409
R_{adj}^2	0.9997	0.9993	0.9989	0.9994	0.9839	0.9826	0.9988	0.9986
F_{error}	0.0327	0.124	0.0631	0.1233	0.216	0.691	0.0741	0.200
				Intraparticle Diffusion				
k_{id} (mg·g^{-1}·h$^{-0.5}$)	0.751[c]	2.13[c]	0.965[c]	2.60[c]	7.13[b]	21.8[b]	9.28[b]	24.2[b]

[a] Conditions: temperature was fixed at 298 K; pH 2.0 biosorbent dosage of 2.5 g·L^{-1}. [b] First stage. [c] Second stage.

macropores (pores with diameters > 50 nm). On the other hand, the number of micropores (pores with a diameter < 2 nm) should be a minimum.[28−30] Usually, the micropore structure is responsible for higher superficial area (S_{BET}) of the materials,[30,47,48] since the nitrogen probe molecule utilized in the measurements is retained basically at the micropore structure.[28−30]

dx.doi.org/10.1021/je100866c |J. Chem. Eng. Data 2011, 56, 1857–1868

Table 5. Isotherm Parameters for RB-5 and RO-16 Biosorption, Using AS and AAS as Biosorbents[a]

	AS		AAS	
	RB-5	RO-16	RB-5	RO-16
	Langmuir			
Q_{max} ($mg \cdot g^{-1}$)	47.6	35.8	55.3	62.9
K_L ($L \cdot mg^{-1}$)	0.0870	0.0513	0.219	0.0618
R_{adj}^2	0.9933	0.9830	0.9407	0.9707
F_{error}	0.968	1.13	3.08	2.87
	Freudlich			
K_F ($mg \cdot g^{-1} \cdot (mg \cdot L^{-1})^{-1/n_F}$)	11.8	4.97	21.5	10.3
n_F	3.59	2.42	4.90	2.63
R_{adj}^2	0.9465	0.9937	0.9713	0.9971
F_{error}	2.74	0.687	2.15	0.900
	Sips			
Q_{max} ($mg \cdot g^{-1}$)	52.3	61.3	72.3	156
K_S ($L \cdot mg^{-1}$)	0.0684	0.0115	0.0957	0.00345
n_S	1.28	1.63	2.06	2.02
R_{adj}^2	0.9999	0.9998	0.9998	0.9995
F_{error}	0.0903	0.114	0.169	0.376

[a] Conditions: temperature was fixed at 298 K; contact time was fixed at (10 and 4) h for AS and AAS, respectively; pH was fixed at 2.0; biosorbent dosage was fixed at 2.5 $g \cdot L^{-1}$.

This explains the low superficial areas (S_{BET}) of the AS and AAS biosorbents.

Effects of Acidity on Adsorption. One of the most important factors in adsorption studies is the effect of the acidity of the medium.[1,2,19,22] Different species may present divergent ranges of suitable pH depending on which adsorbent is used. Effects of initial pH on removal percentage of RB-5 and RO-16 dyes using AS and AAS biosorbents were evaluated within the pH range between (2 and 10) (Figure 2A−D). For both dyes, the percentage of dye removal decreased remarkably from pH 2.0, attaining practically less than 3.2 % and 5.0 % of dye removal at pH 7.5 for AS and AAS, respectively. Similar behavior for dye removal utilizing lignocellulose adsorbents has also been observed.[22,49]

The dissolved RB-5 and RO-16 dyes are negatively charged in water solutions, because they present sulfonate and sulfato-ethyl-sulfone groups.[18,22] The adsorption of these dyes takes place when the biosorbent presents a positive surface charge. At pH 2.0, these lignocellulosic materials presents positive surface charge.[22,49] This behavior explains the high sorption capacity of AS and AAS biosorbents for both RB-5 and RO-16 at pH 2. In order to continue the biosorption studies, the initial pH was fixed at 2.0 for both biosorbents.

Adsorbent Dosage. The study of biosorbent dosages for the removal of RB-5 and RO-16 dyes from aqueous solution was carried out using biosorbent dosages ranging from (1.0 to 10.0) g L^{-1} of AS and AAS, and fixing the initial dye concentration at 40.0 mg L^{-1} and using a time of contact between the adsorbents and adsorbates of 12 h. For both dyes and biosorbents, the highest amount of dye removal was attained for biosorbent doses of at least 2.5 $g \cdot L^{-1}$ (Figure 3A,B for RB-5 and Figure 3C,D for RO-16). For biosorbent dosages higher than this value, the percentage of dye removal remained almost constant. Increases in the percentage of the dye removal with biosorbent dosages up to 2.5 $g \cdot L^{-1}$ could be attributed to increases in the biosorbent surface areas, augmenting the number of adsorption sites available for adsorption, as already reported in several papers.[2,3,15,16,19,31,35,40] On the other hand, the increase in the biosorbent doses promotes a remarkable decrease in the amount of dye uptake per gram of adsorbent (q; Figure 3).

An effect that can be mathematically explained by combining eqs 1 and 2

$$q = \frac{\%\ \text{removal}\ C_o}{100X} \tag{5}$$

As observed from eq 5, the amount of dye uptake (q) and the biosorbent dosage (X) are inversely proportional. For a fixed dye percentage removal, the increase of adsorbent dosage leads to a decrease in q values, since the volume (V) and initial dye concentrations (C_o) are always fixed. These values clearly indicate that the biosorbent dosage must be fixed at 2.5 $g \cdot L^{-1}$, which is the biosorbent dosage that corresponds to the minimum amount of adsorbent that leads to constant dye removal.[1,50]

Kinetic Studies. Adsorption kinetic studies are important in the treatment of aqueous effluents because they provide valuable information on the mechanism of the adsorption process.[31,35]

In attempting to describe the biosorption kinetics of RB-5 and RO-16 dyes by using the AS and AAS biosorbents, four kinetic models were tested, as shown in Figures 4 and 5 for RB-5 and RO-16, respectively. The kinetic parameters for the kinetic models are listed in Table 4. The pseudosecond-order kinetic model presented F_{error} values ranging from 3.00 to 22.3 (RB-5) and from 3.08 to 9.43 (RO-16) times higher the values obtained for the Avrami-fractionary kinetic adsorption model, using both biosorbents. Also, for the pseudofirst-order model, the F_{error} values ranged from 3.36 to 44.7 (RB-5) and from 2.07 to 35.7 (RO-16) times higher than the F_{error} values obtained for the Avrami-fractionary kinetic adsorption model using both biosorbents. The lower the error function, the lower the difference of the q calculated by the model from the experimentally measured q.[1,18,19,44] It should be pointed out that the F_{error} utilized in this work takes into account the number of fitted parameters (p term of eq 4), since it is reported in the literature[51] that depending on the number of parameters a nonlinear equation presents, it has the best fitting of the results. For this reason, the number of fitted parameter should be considered in the calculation of F_{error}. Also, it was verified that the q_e values found in the fractionary-order were closer to the experimental q_e values, when compared with all other kinetic models. These results indicate that the Avrami fractionary-order kinetic model should explain the adsorption process of RB-5 and RO-16 dyes using the AS and AAS biosorbents.

The Avrami kinetic equation has been successfully employed to explain several kinetic processes of different adsorbents and adsorbates.[1−3,16−19,23,30−32,44,52−57] The Avrami exponent (n_{AV}) is a fractionary number related with the possible changes of the adsorption mechanism that takes place during the adsorption process.[30−32] Instead of following only an integer-kinetic order, the mechanism adsorption could follow multiple kinetic orders that are changed during the contact of the adsorbate with the adsorbent.[30−32] The n_{AV} exponent is a result of the multiple kinetic order of the adsorption procedure.[1−3]

Since kinetic results fit very well to the Avrami-fractionary kinetic model for the RB-5 and RO-16 dyes using AS and AAS as biosorbents (Table 4 and Figures 4 and 5), the intraparticle diffusion model[36] was used to verify the influence of mass transfer resistance on the binding of RB-5 and RO-16 dyes to the

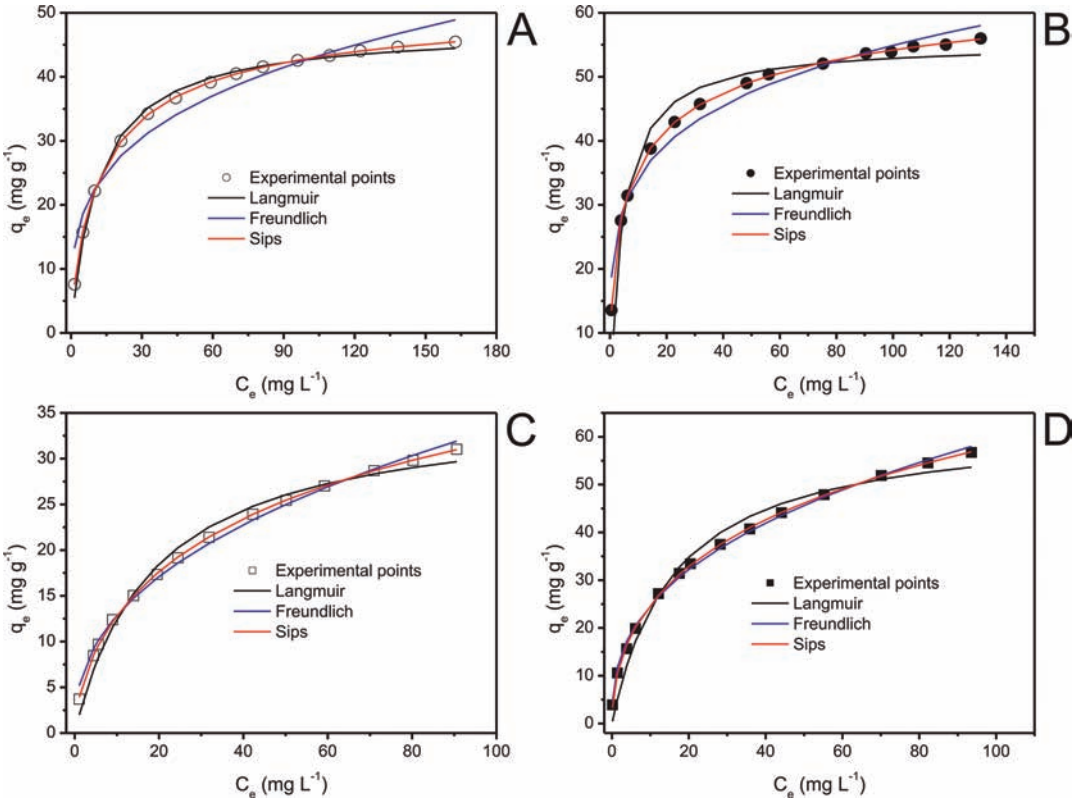

Figure 6. Isotherm curves. (A) RB-5 on AS biosorbent; (B) RB-5 on AAS biosorbent; (C) RO-16 on AS biosorbent; (D) RO-16 on AAS biosorbent. Conditions: pH was fixed at 2.0; the biosorbent dosage was fixed at 2.5 g·L^{-1}; and the temperature was fixed at 298 K. The contact time were fixed at (10 and 4) h for AS and AAS, respectively.

biosorbent (Table 4 and Figure 4B,D,F,H and 5B,D,F,H). The intraparticle diffusion constant, k_{id} (mg·g^{-1}·h$^{-0.5}$), can be obtained from the slope of the plot of q_t (uptaken at any time, mg·g^{-1}) versus the square root of time. These figures show the plots of q_t versus $t^{1/2}$, with multilinearity for the RB-5 and RO-16 dyes using the AS and AAS biosorbents. These results imply that the adsorption processes involve more than one single kinetic stage (or adsorption rate).[35] For the AS biosorbent, the adsorption process exhibits three stages, which can be attributed to each linear portion of the figure (Figures 4B,D and 5B,D). The first linear portion was attributed to the diffusional process of the dye to the CS biosorbent surface;[35] hence, it was the fastest sorption stage. The second portion, ascribed to intraparticle diffusion, was a delayed process. The third stage may be regarded as the diffusion through smaller pores, which is followed by the establishment of equilibrium. For the AAS biosorbent, the adsorption process exhibits only two stages, being the first linear part attributed to intraparticle diffusion, and the second stage the diffusion through smaller pores, which is followed by the establishment of equilibrium.[35]

It was observed in Figures 4 and 5 that the minimum contact time of RB-5 and RO-16 dyes with the AS biosorbent to reach equilibrium was about (8 and 6) h, respectively. For the AAS biosorbent the minimum contact time to attain equilibrium was 2 h for both dyes. This great difference in the minimum contact time to reach equilibrium is associated with the difference in the mechanism of adsorption. These results imply that the diffusion of the dyes from the film could not explain completely the remarkable differences on the kinetics of adsorption of the dyes. As observed in Figures 4 and 5, for the AS biosorbent, three regions were observed in the intraparticle diffusion kinetic graph, on the other hand for the AAS biosorbent, only two linear regions were presented. For the AS biosorbent the film and intraparticle diffusion are rate controlling steps. On the other hand, for the AAS biosorbent, only the intraparticle diffusion is a rate controlling step. This could be confirmed by the intraparticle diffusion constants (k_{id}). The k_{id} for RB-5 and RO-16 were at least 9.5 and 9.6 times, respectively, higher for the AAS biosorbent, when compared with the AS biosorbent. This could explain the difference of (6 and 4) h to reach the equilibrium for RB-5 and RO-16, respectively. This difference in the kinetic behavior is related to differences in the textural properties of the biosorbents after the treatment with acid, as already reported in the literature,[17,18,22,23] and also in agreement with the results discussed above in the characterization of the biosorbents.

In order to continue this work, the contact time between the biosorbents and biosorbates were fixed at (10.0 and 4.0) h using the AS and AAS biosorbents, respectively, for both dyes as biosorbates. This increase in the contact time utilized in this work was to guarantee that for both dyes equilibrium would be attained even at higher biosorbate concentrations.

Equilibrium Studies. An adsorption isotherm describes the relationship between the amount of adsorbate taken up by the adsorbent (q_e) and the adsorbate concentration remaining in the solution after the system attained the equilibrium (C_e). There are several equations to analyze experimental adsorption equilibrium data. The equation parameters of these equilibrium models often provide some insight into the adsorption mechanism, the surface properties and affinity of the adsorbent. In this work, the Langmuir,[36] the Freundlich,[37] and the Sips[38] isotherm models were tested.

Table 6. Comparison of Maxima Adsorption Capacities for RB-5 and RO-16 Adsorbed[a]

adsorbent	Q_{max} (mg·g^{-1}) RB-5	RO-16	ref
carbonized Brazilian pine-fruit shell (C-PW)		320	15
activated carbon from Brazilian pine-fruit shell (AC-PW)		472	15
waterworks sludge		86.8	58
sewage sludge		47.0	58
landfill sludge		114.7	58
polysulfone-immobilized protonated *C. glutamicum* biomass		94.4	59
chitosan cross-linked (beads)		30	60
chitosan cross-linked (beads)		5.6	60
chitosan		30.4	61
chitosan hydrogel beads	709.3		62
chitosan hydrogel beads	413.2		62
high lime fly ash	7.18		63
cetyltrimethylammonium bromide modified zeolite	12.9		64
powdered activated carbon	58.52		65
fly ash	7.93		65
bone char	157		66
brown seaweed, Laminaria sp	101.5		67
aqai stalk (AS)	52.3	61.3	this work
acidified aqai stalk (AAS)	72.3	156	this work

[a] The values were obtained at the best experimental conditions of each work.

Table 7. Molecular Properties of RB-5 and RO-16 Calculated by the Software ChemBio 3D Ultra Version 11.0

properties	RB-5	RO-16	ratio RB-5/RO-16
Connolly accessible area/nm^2	11.36	7.71	1.47
Connolly molecular area/nm^2	6.42	4.20	1.53
Connolly solvent excluded volume/nm^3	5.86	3.70	1.58

The isotherms of adsorption of RB-5 and RO-16 were carried out at 298 K on the AS and AAS biosorbents, using the best experimental conditions described previously (see Table 5 and Figure 6). Based on the F_{error}, the Sips model is the best isotherm model for both dyes and biosorbents. The maximum amounts of RB-5 and RO-16 adsorbed were (52.3 and 61.3) mg·g^{-1}, respectively, using AS as the biosorbent and (72.3 and 156) mg·g^{-1}, respectively using AAS as the biosorbent.

These values indicate that AS and AAS are fairly good biosorbents for the removal of these dyes from aqueous solutions (see Table 6).[15,58−67] For the RB-5 dye, out of ten different adsorbents, AAS presents an adsorption capacity higher than 5, and for RO-16 dye, out of eleven different adsorbents, AAS presents an adsorption capacity higher than eight.

It should be highlighted that the maximum amount adsorbed (Q_{max}) of the RB-5 and RO-16 dyes by the biosorbents was 1.38 and 2.54-fold respectively, higher for the AAS biosorbent when compared with the AS biosorbent. Considering that the kinetics of adsorption of both dyes were also faster using the AAS biosorbent (see Table 4), it can be concluded that the acid treatment of aqai stalk promoted the increase of macropore structure on the biomaterial (see Figure 1), contributing to a faster diffusion of the dyes through the pores of the biosorbent, and also allowing higher amounts of the dyes to be adsorbed by the AAS biosorbent. This effect was more pronounced for the RO-16 dye than for RB-5, since the maximum longitudinal length of RB-5 is 2.55 nm, whereas this value for RO-16 is only 1.68 nm (see the Supporting Information, Figure 1). In Table 7 are presented molecular properties of RB-5 and RO-16 dyes calculated by the Sofware ChemBio 3D Ultra version 11.0. According to these values, the Connolly solvent excluded volume of RB-5 is 58% higher than the RO-16 dye, and also the Connolly molecular area and accessible area of the RB-5 dye is higher when compared with the RO-16 dye. The lower is the volume of the dye molecule, the faster is the kinetics of adsorption (see Table 4) and also easier is the arrangement of the dye molecules on the external and internal part of the biosorbent, because lower will be the steric hindrance caused by the adsorbed dye molecule.[68] Therefore, it is expected that smaller dye molecules will allow higher adsorption capacity.

CONCLUSION

The aqai palm stalk (*Euterpe oleracea*) in natural form (AS) as well as a protonated form (AAS) are good alternative biosorbents to remove the textile dyes C.I. Reactive Black 5 (RB-5) and C.I. Reactive Orange 16 (RO-16) from aqueous solutions. The AS and AAS were characterized by FTIR spectroscopy, SEM, and nitrogen adsorption/desorption curves. It was demonstrated that the OH groups of phenols and alcohols and carboxylate groups presented a shift to lower wavenumbers after contact with both dyes, indicating that these groups should participate in the biosorption mechanism. Both dyes interact with the biosorbents at the solid/liquid interface when suspended in water. The best conditions were established with respect to pH and contact time to saturate the available sites located on the adsorbent surface. Four kinetic models were used to adjust the adsorption and the best fit was obtained with the Avrami (fractionary-order) kinetic model. However, the intraparticle diffusion model gave multiple

linear regions, which suggested that the biosorption may also be followed by multiple adsorption rates. The equilibration time of both dyes were obtained after (10 and 4) h of contact between the dyes and the AS and AAS biosorbents, respectively. The shorter time of contact for AAS biosorbent was attributed to the macropores generated at the aqai fiber after acid treatement. The equilibrium isotherm of these dyes was obtained, that were best fitted to the Sips isotherm model. The maximum amounts of RB-5 and RO-16 adsorbed were (52.3 and 61.3) $mg \cdot g^{-1}$, respectively, using AS as biosorbent and (72.3 and 156) $mg \cdot g^{-1}$, respectively using AAS as biosorbent.

■ ASSOCIATED CONTENT

Supporting Information. Structural formulae of RB-5 and RO-16 and additional FTIR spectra. This material is available free of charge via the Internet at http://pubs.acs.org.

■ AUTHOR INFORMATION

Corresponding Author

*Fax: +55 (51) 3308-7304. Phone: +55 (51) 3308 7175. E-mail: eder.lima@ufrgs.br; profederlima@gmail.com.

Funding Sources

The authors are grateful to CNPq, to CAPES and to FAPERGS for financial support and fellowships.

■ ACKNOWLEDGMENT

We are grateful to Centro de Microscopia Eletrônica (CME-UFRGS) for the use of the SEM microscope.

■ NOMENCLATURE

C constant related with the thickness of boundary layer $(mg \cdot g^{-1})$
C_e dye concentration at the equilibrium $(mg \cdot L^{-1})$
C_f dye concentration at ending of the adsorption $(mg \cdot L^{-1})$
C_o initial dye concentration put in contact with the adsorbent $(mg \cdot L^{-1})$
h_o the initial sorption rate $(mg \cdot g^{-1} \cdot h^{-1})$
k_{AV} is the Avrami kinetic constant $[(h^{-1})]$
K_F the Freundlich equilibrium constant $[mg \cdot g^{-1} \cdot (mg \cdot L^{-1})^{-1/nF}]$
k_f the pseudofirst order rate constant (h^{-1})
k_{id} the intraparticle diffusion rate constant $(mg \cdot g^{-1} \cdot h^{-0.5})$
K_L the Langmuir equilibrium constant $(L \cdot mg^{-1})$
K_S the Sips equilibrium constant $(L \cdot mg^{-1})$
k_s the pseudosecond order rate constant $(g \cdot mg^{-1} \cdot h^{-1})$
n_{AV} is a fractionary reaction order (Avrami) which can be related, to the adsorption mechanism
n_F dimensionless exponent of the Freundlich equation
n_S dimensionless exponent of the Sips equation
q amount adsorbed of the dye by the adsorbent $(mg \cdot g^{-1})$
q_e amount adsorbate adsorbed at the equilibrium $(mg \cdot g^{-1})$
Q_{max} the maximum adsorption capacity of the adsorbent $(mg \cdot g^{-1})$
q_t amount of adsorbate adsorbed at time $(mg \cdot g^{-1})$
t time of contact (h)
X biosorbent dosage $(g \cdot L^{-1})$

■ REFERENCES

(1) Cardoso, N. F.; Pinto, R. B.; Lima, E. C.; Calvete, T.; Amavisca, C. V.; Royer, B.; Cunha, M. L.; Fernandes, T. H. M.; Pinto, I. S. Removal of remazol black B textile dye from aqueous solution by adsorption. *Desalination* **2011**, *269*, 92–103.

(2) Royer, B.; Cardoso, N. F.; Lima, E. C.; Ruiz, V. S. O.; Macedo, T. R.; Airoldi, C. Organofunctionalized kenyaite for dye removal from aqueous solution. *J. Colloid Interface Sci.* **2009**, *336*, 398–405.

(3) Royer, B.; Cardoso, N. F.; Lima, E. C.; Macedo, T. R.; Airoldi, C. Sodic and acidic crystalline lamellar magadiite adsorbents for removal of methylene blue from aqueous solutions. Kinetic and equilibrium studies. *Sep. Sci. Technol.* **2010**, *45*, 129–141.

(4) Brookstein, D. S. Factors associated with textile pattern dermatitis caused by contact allergy to dyes, finishes, foams, and preservatives. *Dermatol. Clin.* **2009**, *27*, 309–322.

(5) de Lima, R. O. A.; Bazo, A. P.; Salvadori, D. M. F.; Rech, C. M.; Oliveira, D. P.; Umbuzeiro, G. A. Mutagenic and carcinogenic potential of a textile azo dye processing plant effluent that impacts a drinking water source. *Mutat. Res. Genet. Toxicol. Environ. Mutagen.* **2007**, *626*, 53–60.

(6) Carneiro, P. A.; Umbuzeiro, G. A.; Oliveira, D. P.; Zanoni, M. V. B. Assessment of water contamination caused by a mutagenic textile effluent/dyehouse effluent bearing disperse dyes. *J. Hazard. Mater.* **2010**, *174*, 694–699.

(7) Riera-Torres, M.; Gutiérrez-Bouzán, C.; Crespi, M. Combination of coagulation−flocculation and nanofiltration techniques for dye removal and water reuse in textile effluents. *Desalination* **2010**, *252*, 53–59.

(8) Anandan, S.; Lee, G. J.; Chen, P. K.; Fan, C.; Wu, J. J. Removal of Orange II Dye in Water by Visible Light Assisted Photocatalytic Ozonation Using Bi_2O_3 and Au/Bi_2O_3 Nanorods. *Ind. Eng. Chem. Res.* **2010**, *49*, 9729–9737.

(9) Berberidou, C.; Avlonitis, S.; Poulios, I. Dyestuff effluent treatment by integrated sequential photocatalytic oxidation and membrane filtration. *Desalination* **2009**, *249*, 1099–1106.

(10) Liang, X.; Zhong, Y.; Zhu, S.; Zhu, J.; Yuan, P.; He, H.; Zhang, J. The decolorization of Acid Orange II in non-homogeneous Fenton reaction catalyzed by natural vanadium−titanium magnetite. *J. Hazard. Mater.* **2010**, *181*, 112–120.

(11) Zhang, Y.; Li, D.; Chen, Y.; Wang, X.; Wang, S. Catalytic wet air oxidation of dye pollutants by polyoxomolybdate nanotubes under room condition. *Appl. Catal., B* **2009**, *86*, 182–189.

(12) Raghu, S.; Lee, C. W.; Chellammal, S.; Palanichamy, S.; Basha, C. A. Evaluation of electrochemical oxidation techniques for degradation of dye effluents—A comparative approach. *J. Hazard. Mater.* **2009**, *171*, 748–754.

(13) Novotný, Č.; Svobodová, K.; Benada, O.; Kofroňová, O.; Heissenberger, A.; Fuchs, W. Potential of combined fungal and bacterial treatment for color removal in textile wastewater. *Bioresour. Technol.* **2011**, *102*, 879–888.

(14) Forgacs, E; Cseháti, T; Oros, G. Removal of synthetic dyes from wastewaters: a review. *Environ. Int.* **2004**, *30*, 953–971.

(15) Royer, B.; Lima, E. C.; Cardoso, N. F.; Calvete, T.; Bruns, R. E. Statistical design of experiments for optimization of batch adsorption conditions for removal of reactive red 194 textile dye from aqueous effluents. *Chem. Eng. Commun.* **2010**, *197*, 775–790.

(16) Royer, B.; Cardoso, N. F.; Lima, E. C.; Macedo, T. R.; Airoldi, C. A useful organofunctionalized layered silicate for textile dye removal. *J. Hazard. Mater.* **2010**, *181*, 366–374.

(17) Calvete, T.; Lima, E. C.; Cardoso, N. F.; Dias, S. L. P.; Pavan, F. A. Application of carbon adsorbents prepared from the Brazilian-pine fruit shell for removal of Procion Red MX 3B from aqueous solution - Kinetic, equilibrium, and thermodynamic studies. *Chem. Eng. J.* **2009**, *155*, 627–636.

(18) Calvete, T; Lima, E. C.; Cardoso, N. F.; Vaghetti, J. C. P.; Dias, S. L. P.; Pavan, F. A. Application of carbon adsorbents prepared from Brazilian-pine fruit shell for the removal of reactive orange 16 from aqueous solution: Kinetic, equilibrium, and thermodynamic studies. *J. Environ. Manage.* **2010**, *91*, 1695–1706.

(19) Calvete, T; Lima, E. C.; Cardoso, N. F.; Dias, S. L. P.; Ribeiro, E. S. Removal of Brilliant Green Dye from Aqueous Solutions Using Home Made Activated Carbons. *Clean: Soil, Air, Water* **2010**, *38*, 521–532.

(20) Crini, G. Non-conventional low-cost adsorbents for dye removal: A review. *Bioresour. Technol.* **2006**, *97*, 1061–1085.

(21) Gupta, V. K.; Suhas, I. A. Application of low-cost adsorbents for dye removal − A review. *J. Environ. Manage.* **2009**, *90*, 2313–2342.

(22) Lima, E. C.; Royer, B.; Vaghetti, J. C. P.; Simon, N. M.; da Cunha, B. M.; Pavan, F. A.; Benvenutti, E. V.; Veses, R. C.; Airoldi, C. Application of Brazilian-pine fruit coat as a biosorbent to removal of reactive red 194 textile dye from aqueous solution, Kinetics and equilibrium study. *J. Hazard. Mater.* **2008**, *155*, 536–550.

(23) Royer, B.; Cardoso, N. F.; Lima, E. C.; Vaghetti, J. C. P.; Simon, N. M.; Calvete, T.; Veses, R. C. Applications of Brazilian-pine fruit shell in natural and carbonized forms as adsorbents to removal of methylene blue from aqueous solutions - Kinetic and equilibrium study. *J. Hazard. Mater.* **2009**, *164*, 1213–1222.

(24) Açai Farms, http://www.acaifarms.com/, website visited on January 6th, 2010.

(25) Pacheco-Palencia, L. A.; Duncan, C. E.; Talcott, S. T. Phytochemical composition and thermal stability of two commercial açai species, *Euterpe oleracea* and *Euterpe precatoria*. *Food Chem.* **2009**, *115*, 1199–1205.

(26) Açai Palm- Wikipedia, http://en.wikipedia.org/wiki/A%C3%A7ai, website visited on January 6th, 2011.

(27) de Vasconcelos, M. A. M.; Alves, S. M. Production system of Açai, http://sistemasdeproducao.cnptia.embrapa.br/FontesHTML/Acai/SistemaProducaoAcai_2ed/paginas/intro.htm, website visited on August 21st, 2010.

(28) Arenas, L. T.; Lima, E. C.; dos Santos, A. A., Jr.; Vaghetti, J. C. P.; Costa, T. M. H.; Benvenutti, E. V. Use of statistical design of experiments to evaluate the sorption capacity of 1,4-diazoniabicyclo-[2.2.2]octane/silica chloride for Cr(VI) adsorption. *Colloids Surf. A* **2007**, *297*, 240–248.

(29) Jacques, R. A.; Bernardi, R.; Caovila, M.; Lima, E. C.; Pavan, F. A.; Vaghetti, J. C. P.; Airoldi, C. Removal of Cu(II), Fe(III) and Cr(III) from aqueous solution by aniline grafted silica gel. *Sep. Sci. Technol.* **2007**, *42*, 591–609.

(30) Gay, D. S. F.; Fernandes, T. H. M.; Amavisca, C. V.; Cardoso, N. F.; Benvenutti, E. V.; Costa, T. M. H.; Lima, E. C. Silica grafted with a silsesquioxane containing the positively charged 1,4-diazoniabicyclo-[2.2.2]octane group used as adsorbent for anionic dye removal. *Desalination* **2010**, *258*, 128–135.

(31) Vaghetti, J. C. P.; Lima, E. C.; Royer, B.; Cardoso, N. F.; Martins, B.; Calvete, T. Pecan nutshell as biosorbent to remove toxic metals from aqueous solution. *Sep. Sci. Technol.* **2009**, *44*, 615–644.

(32) Lopes, E. C. N.; dos Anjos, F. S. C.; Vieira, E. F. S.; Cestari, A. R. An alternative Avrami equation to evaluate kinetic parameters of the interaction of Hg(II) with thin chitosan membranes. *J. Colloid Interface Sci.* **2003**, *263*, 542–547.

(33) Largegren, S. About the theory of so-called adsorption of soluble substances. *Kungliga Suensk Vetenskapsakademiens Handlingar* **1898**, *241*, 1–39.

(34) Ho, Y. S.; Mckay, G. M. Pseudo-second order model for sorption process. *Proc. Biochem.* **1999**, *34*, 451–465.

(35) Weber, W. J., Jr.; Morris, J. C. Kinetics of adsorption on carbon from solution. *J. Sanit. Eng. Div. Am. Soc. Civil Eng.* **1963**, *89*, 31–59.

(36) Langmuir, I. The adsorption of gases on plane surfaces of glass, mica and platinum. *J. Am. Chem. Soc.* **1918**, *40*, 1361–1403.

(37) Freundlich, H. Adsorption in solution. *Phys. Chem. Soc.* **1906**, *40*, 1361–1368.

(38) Sips, R. On the structure of a catalyst surface. *J. Chem. Phys.* **1948**, *16*, 490–495.

(39) Vaghetti, J. C. P.; Lima, E. C.; Royer, B.; Brasil, J. L.; da Cunha, B. M.; Simon, N. M.; Cardoso, N. F.; Noreña, C. P. Z. Application of Brazilian-pine fruit coat as a biosorbent to removal of Cr(VI) from aqueous solution. Kinetics and equilibrium study. *Biochem. Eng. J.* **2008**, *42*, 67–76.

(40) Lima, E. C.; Barbosa, F., Jr; Krug, F. J.; Tavares, A. Copper determination in biological materials by ETAAS using W-Rh permanent modifier. *Talanta* **2002**, *57*, 177–186.

(41) Lima, E. C.; Fenga, P. G.; Romero, J. R.; de Giovani, W. F. Electrochemical behaviour of $[Ru(4,4'\text{-}Me_2bpy)_2(PPh_3)(H_2O)](ClO_4)_2$ in homogeneous solution and incorporated into carbon paste electrodes. Application to oxidation of benzylic compounds. *Polyhedron* **1998**, *17*, 313–318.

(42) Lima, E. C.; Krug, F. J.; Nobrega, J. A.; Nogueira, A. R. A. Determination of ytterbium in animal faeces by tungsten coil electrothermal atomic absorption spectrometry. *Talanta* **1998**, *47*, 613–623.

(43) Lima, E. C.; Royer, B.; Vaghetti, J. C. P.; Brasil, J. L.; Simon, N. M.; dos Santos, A. A., Jr.; Pavan, F. A.; Dias, S. L. P.; Benvenutti, E. V.; da Silva, E. A. Adsorption of Cu(II) on Araucaria angustifolia wastes: Determination of the optimal conditions by statistic design of experiments. *J. Hazard. Mater.* **2007**, *140*, 211–220.

(44) Vaghetti, J. C. P.; Lima, E. C.; Royer, B.; da Cunha, B. M.; Cardoso, N. F.; Brasil, J. L.; Dias, S. L. P. Pecan nutshell as biosorbent to remove Cu(II), Mn(II) and Pb(II) from aqueous solutions. *J. Hazard. Mater.* **2009**, *162*, 270–280.

(45) Smith, B. *Infrared spectral Interpretation − A systematic approach*; CRC Press: Boca Raton, FL, 1999.

(46) Kara, S.; Aydiner, C.; Demirbas, E.; Kobya, M.; Dizge, N. Modeling the effects of adsorbent dose and particle size on the adsorption of reactive textile dyes by fly ash. *Desalination* **2007**, *212*, 282–293.

(47) Kumari, P.; Sharma, P.; Srivastava, S.; Srivastava, M. M. Biosorption studies on shelled Moringa oleifera Lamarck seed powder: Removal and recovery of arsenic from aqueous system. *Int. J. Miner. Process* **2006**, *78*, 131–139.

(48) Yurtsever, M.; Sengil, I. A. Biosorption of Pb(II) ions by modified quebracho tannin resin. *J. Hazard. Mater.* **2009**, *163*, 58–64.

(49) Deniz, F.; Saygideger, S. D. Equilibrium, kinetic and thermodynamic studies of Acid Orange 52 dye biosorption by Paulownia tomentosa Steud. leaf powder as a low-cost natural biosorbent. *Bioresour. Technol.* **2010**, *101*, 5137–5143.

(50) Oladoja, N. A.; Akinlabi, A. K. Congo Red Biosorption on Palm Kernel Seed Coat. *Ind. Eng. Chem. Res.* **2009**, *48*, 6188–6196.

(51) El-Khaiary, M. I.; Malash, G. F. Common data analysis errors in batch adsorption studies. *Hydrometallurgy* **2011**, *105*, 314–320.

(52) Cestari, A. R.; Vieira, E. F. S.; Pinto, A. A.; Lopes, E. C. N. Multistep adsorption of anionic dyes on silica/chitosan hybrid 1. Comparative kinetic data from liquid- and solid-phase models. *J. Colloid Interface Sci.* **2005**, *292*, 363–372.

(53) Cestari, A. R.; Vieira, E. F. S.; Vieira, G. S.; Almeida, L. E. The removal of anionic dyes from aqueous solutions in the presence of anionic surfactant using aminopropylsilica. -A kinetic study. *J. Hazard. Mater.* **2006**, *138*, 133–141.

(54) Bascialla, G.; Regazzoni, A. E. Immobilization of anionic dyes by intercalation into hydrotalcite. *Colloids Surf. A* **2008**, *328*, 34–39.

(55) Zubieta, C. E.; Messina, P. V.; Luengo, C.; Dennehy, M.; Pieroni, O.; Schulz, P. C. Reactive dyes remotion by porous TiO_2-chitosan materials. *J. Hazard. Mater.* **2008**, *152*, 765–777.

(56) Serna-Guerrero, R.; Sayari, A. Modeling adsorption of CO_2 on amine-functionalized mesoporous silica. 2: Kinetics and breakthrough curves. *Chem. Eng. J.* **2010**, *161*, 182–190.

(57) Cardoso, N. F.; Lima, E. C.; Pinto, I. S.; Amavisca, C. V.; Royer, B.; Pinto, R. B.; Alencar, W. S.; Pereira, S. F. P. Application of cupuassu shell as biosorbent for the removal of textile dyes from aqueous solution. *J. Environ. Manage.* **2011**, *92*, 1237–1247.

(58) Won, S. W.; Choi, S. B.; Yun, Y. S. Performance and mechanism in binding of Reactive Orange 16 to various types of sludge. *Biochem. Eng. J.* **2006**, *28*, 208–214.

(59) Vijayaraghavan, K.; Yun, Y. S. Competition of Reactive red 4, Reactive orange 16 and Basic blue 3 during biosorption of Reactive blue 4 by polysulfone-immobilized *Corynebacterium glutamicum*. *J. Hazard. Mater.* **2008**, *153*, 478–486.

(60) Kimura, I. Y.; Laranjeira, M. C. M.; Fávere, V. T.; Furlan, L. The interaction between reactive dye containing vinylsulfone group and chitosan microspheres. *Int. J. Polym. Mater.* **2002**, *51*, 759–768.

(61) Crini, G.; Badot, P. M. Application of chitosan, a natural aminopolysaccharide, for dye removal from aqueous solutions by adsorption processes using batch studies: A review of recent literature. *Prog. Polym. Sci.* **2008**, *33*, 399–447.

(62) Chatterjee, S.; Chatterjee, T.; Woo, S. H. Influence of the polyethyleneimine grafting on the adsorption capacity of chitosan beads for Reactive Black 5 from aqueous solutions. *Chem. Eng. J.* **2011**, *166*, 168–175.

(63) Eren, Z.; Acar, F. N. Equilibrium and kinetic mechanism for Reactive Black 5 sorption onto high lime Soma fly ash. *J. Hazard. Mater.* **2007**, *143*, 226–232.

(64) Karadag, D.; Turan, M.; Akgul, E.; Tok, S.; Faki, A. Adsorption equilibrium and kinetics of Reactive Black 5 and Reactive Red 239 in aqueous solution onto surfactant-modified zeolite. *J. Chem. Eng. Data* **2007**, *52*, 1615–1620.

(65) Eren, Z.; Acar, F. N. Adsorption of Reactive Black 5 from an aqueous solution: equilibrium and kinetic studies. *Desalination* **2006**, *194*, 1–10.

(66) Ip, A. W. M.; Barford, J. P.; McKay, G. Reactive Black dye adsorption/desorption onto different adsorbents: effect of salt, surface chemistry, pore size and surface area. *J. Colloid Interface Sci.* **2009**, *337*, 32–38.

(67) Vijayaraghavan, K.; Yun, Y. S. Biosorption of C.I. Reactive Black 5 from aqueous solution using acid-treated biomass of brown seaweed Laminaria sp. *Dyes Pigm.* **2008**, *76*, 726–732.

(68) Vachoud, L.; Zydowicz, N.; Domard, A. Sorption and desorption studies on chitin gels. *Int. J. Biol. Macromol.* **2001**, *28*, 93–101.